Fibroblast Growth Factor 21 Mediates Specific Glucagon Actions

Kirk M. Habegger,[1] Kerstin Stemmer,[2] Christine Cheng,[3] Timo D. Müller,[2] Kristy M. Heppner,[1] Nickki Ottaway,[1] Jenna Holland,[1] Jazzminn L. Hembree,[1] David Smiley,[4] Vasily Gelfanov,[4] Radha Krishna,[1] Ayman M. Arafat,[5] Anish Konkar,[6] Sara Belli,[6] Martin Kapps,[6] Stephen C. Woods,[1] Susanna M. Hofmann,[7] David D'Alessio,[1] Paul T. Pfluger,[2] Diego Perez-Tilve,[1] Randy J. Seeley,[1] Morichika Konishi,[8] Nobuyujki Itoh,[8] Alexei Kharitonenkov,[3] Joachim Spranger,[5] Richard D. DiMarchi,[4] and Matthias H. Tschöp[2]

Glucagon, an essential regulator of glucose homeostasis, also modulates lipid metabolism and promotes weight loss, as reflected by the wasting observed in glucagonoma patients. Recently, coagonist peptides that include glucagon agonism have emerged as promising therapeutic candidates for the treatment of obesity and diabetes. We developed a novel stable and soluble glucagon receptor (GcgR) agonist, which allowed for in vivo dissection of glucagon action. As expected, chronic GcgR agonism in mice resulted in hyperglycemia and lower body fat and plasma cholesterol. Notably, GcgR activation also raised hepatic expression and circulating levels of fibroblast growth factor 21 (FGF21). This effect was retained in isolated primary hepatocytes from wild-type (WT) mice, but not GcgR knockout mice. We confirmed this link in healthy human volunteers, where injection of natural glucagon increased plasma FGF21 within hours. Functional relevance was evidenced in mice with genetic deletion of *FGF21*, where GcgR activation failed to induce the body weight loss and lipid metabolism changes observed in WT mice. Taken together, these data reveal for the first time that glucagon controls glucose, energy, and lipid metabolism at least in part via FGF21-dependent pathways. ***Diabetes*** **62:1453–1463, 2013**

Released during periods of hypoglycemia, glucagon is the key counter-regulatory hormone opposing insulin action. Identified in the 1920s, glucagon is secreted by pancreatic α-cells (1) and encoded by the proglucagon gene. Glucagon is best known for its stimulation of hepatic glucose production by increasing glycogenolysis and gluconeogenesis, while simultaneously inhibiting glycogen synthesis. Accordingly, unopposed glucagon signaling is a crucial pathophysiological component of diabetes and thus has been widely studied (2–6). However, glucagon action regulates a far greater range of physiological processes, including lipolysis, ketogenesis, fatty acid oxidation, satiation, thermogenesis, energy expenditure (EE), and bile acid metabolism. Recent studies have revealed that when coupled with glucagon-like protein 1 (GLP-1) agonism, glucagon action may offer previously unrecognized therapeutic opportunities for the metabolic syndrome (7,8). Although such provocative findings have renewed interest in glucagon research, the molecular underpinnings of these effects remained elusive.

Glucagon is only one of several fasting hormones. It is thus possible that one, or several, other hormone(s) with a metabolic role during fasting is regulated by, or mediates a portion of, glucagon's effects. Among these fasting-induced hormones is fibroblast growth factor 21 (FGF21), which has recently received considerable attention (9). FGF21 expression and secretion are elicited in the liver during periods of fasting (10–12) and may be induced by downstream signaling of glucagon (8,13). Recent studies suggest that, like glucagon, FGF21 signaling regulates glucose, lipid, cholesterol, and bile acid metabolism (14,15), implicating FGF21 as an attractive drug candidate for metabolic disease. We report here that FGF21 mediates the key metabolic actions of glucagon.

RESEARCH DESIGN AND METHODS

Synthesis of a novel glucagon receptor agonist (IUB288). 0.2 mmol Boc Thr(Bzl)-Pam resin was the initial synthetic substrate upon which the target peptide was assembled through repetitive DEPBT/diisopropylethylamine (DIEA) activated single couplings on a CSBio336 peptide synthesizer (7). The assembled peptide resin was treated with 20% piperidine/dimethylformamide (DMF) at room temperature for 10 min to remove the side-chain Fmoc protection. The resin was filtered and washed with DMF, and an activated solution of Fmoc Glu-αOBzl was added to acylate the Lys10 side chain (previously prepared by dissolving FmocGlu-αBzl[Aapptec] in 0.5 mol/L DEPBT/DMF and subsequently adding DIEA). After 1 h, the resin was filtered and washed with DMF. The above process was repeated using an equivalent aliquot of Fmoc Glu-αOBzl and once more with 2.0 mmol palmitic acid (Sigma, St. Louis, MO). The completed peptide resin was filtered, washed, treated with 50% trifluoroacetic acid/dichloromethane, and neutralized with 5% DIEA/dichloromethane. The peptide was cleaved from the resin in liquid hydrogen fluid in the presence of *p*-cresol at 0°C, for 1 h. The peptide was solubilized in 50% aqueous acetonitrile, diluted with dilute ammonium bicarbonate, and purified by Amberchrom XT20 chromatography with a linear gradient of aqueous acetonitrile in 0.025 mol/L ammonium bicarbonate. The pure peptide of the sequence HaibQGTFISDK(rErE-C16)SKYLDaibRAAQDFVQWLMDT was identified by analytical high-performance liquid chromatography and electrospray ionization mass spectral analysis; theoretical molecular weight = 3,868.4 g/mol and observed mass = 3,867.5 g/mol.

From the [1]Metabolic Disease Institute, Division of Endocrinology, Diabetes, and Metabolism, Department of Medicine, University of Cincinnati, Cincinnati, Ohio; the [2]Institute for Diabetes and Obesity, Helmholtz Zentrum München and Technische Universität München, Munich, Germany; [3]Diabetes Research, Lilly Research Laboratories, Lilly Corporate Center, Indianapolis, Indiana; the [4]Department of Chemistry, Indiana University, Bloomington, Indiana; the [5]Department of Endocrinology, Diabetes, and Nutrition, Charité University Hospitals, Berlin, Germany; [6]F. Hoffmann-La Roche Ltd., Basel, Switzerland; the [7]Institute of Experimental Genetics, Helmholtz Zentrum München, German Research Center for Environmental Health, München/Neuherberg, Germany; and the [8]Department of Genetic Biochemistry, Kyoto University Graduate School of Pharmaceutical Sciences, Sakyo, Kyoto, Japan.

Corresponding author: Matthias H. Tschöp, matthias.tschoep@helmholtz-muenchen.de.

Received 17 August 2012 and accepted 19 November 2012.

DOI: 10.2337/db12-1116

This article contains Supplementary Data online at http://diabetes.diabetesjournals.org/lookup/suppl/doi:10.2337/db12-1116/-/DC1.

See accompanying commentary, p. 1376.

Reporter gene assay. The relative receptor potency at the glucagon and GLP-1 receptor was determined by the ability of IUB288 to induce cAMP and was measured in a firefly luciferase-based reporter gene assay as previously described (7). In brief, HEK293 cells cotransfected with either glucagon or the GLP-1 receptor and the luciferase gene linked to the cAMP-responsive element were used (7). The cells were serum deprived by culturing for 16 h in Dulbecco's modified Eagle's medium (Invitrogen, Carlsbad, CA) supplemented with 0.25% bovine growth serum (HyClone, Logan, UT) and then incubated with serial dilutions of either glucagon, GLP-1, or IUB288 for 5 h at 37°C, 5% CO_2 in 96-well poly-D-lysine–coated Biocoat plates (BD Biosciences, San Jose, CA). At the end of the incubation, 100 μL of LucLite luminescence substrate reagent (Perkin Elmer, Wellesley, MA) was added to each well. The plate was shaken briefly and incubated for 10 min in the dark, and light output was measured on a MicroBeta-1450 liquid scintillation counter (PerkinElmer, Wellesley, MA).

Glucagon challenge in man. In a double-blind crossover design, obese healthy subjects (five men: 29.4 ± 2.6 years of age and BMI = 33.9 ± 1.6 kg/m^2) received 1 mg of glucagon (GlucaGen; Novo Nordisk Pharma Inc., Bagsværd, Denmark) intramuscularly. The test was performed as detailed previously (16). Serum FGF21 levels were determined by radioimmunoassay (Phoenix Europe GmbH, Karlsruhe, Germany).

Animal models. FGF21-deficient mice were generated as previously described (17) and maintained in our facilities on a C57Bl/6J (Jackson Laboratories) background. All mice were fed a standard chow (Teklad LM-485, 5.6% fat) or high-fat diet (HFD; 58.0 kcal % fat; D12331 Research Diets, New Brunswick, NJ). *db/db* mice were obtained from Jackson Laboratories. Glucagon receptor (GcgR)–deficient mice were obtained from Deltagene (San Mateo, CA). Mice were single or group housed on a 12:12-h light-dark cycle (light on from 0600 to 1800 h) at 22°C and constant humidity with free access to food and water, except as noted. All studies were approved by and performed according to the guidelines of the Institutional Animal Care and Use Committee of the University of Cincinnati.

Body composition measurements. Whole-body composition (fat and lean mass) was measured using noninvasive nuclear magnetic resonance technology (EchoMRI, Houston, TX).

IUB288 pharmacokinetics. Two male C57Bl/6J mice were fasted and then injected subcutaneously with 10 nmol/kg IUB288. Plasma samples were collected 1, 3, 5, 7, and 24 h after injection, and IUB288 concentrations were determined by liquid chromatography–mass spectrometry, pharmacokinetics calculations by Biobook (IDBS e-workbook Suite 8.2.0).

Glucose and insulin tolerance tests. Intraperitoneal glucose and insulin tolerance tests were performed by injection of glucose (2 g/kg, 20% wt/vol D-glucose [Sigma] in 0.9% wt/vol saline) or human regular insulin (0.75 units/kg [Lilly Humalog] in 0.9% wt/vol saline) to 6-h fasted mice. Blood samples were collected immediately before and 15, 30, 45, 60, 90, and 120 min after injection. Blood glucose was determined with a TheraSense Freestyle glucometer.

Hormone measurements. Plasma insulin, GLP-1, and glucagon were determined using Meso Scale Discovery MULTI-ARRAY Assay System (Meso Scale Discovery, Gaithersburg, MD). IUB288 concentrations from 0.2 pmol/mL to 200 nmol/mL were undetectable using this assay (data not shown), suggesting that there was no cross-reactivity with the injected compound. Plasma FGF21 was analyzed individually by ELISA assay (EZRMFGF21–26 K; Millipore, Billerica, MA). Plasma leptin was measured via Luminex. Plasma triglycerides, nonesterified free fatty acids (NEFAs), ketone bodies, and cholesterol levels were analyzed individually by enzymatic assay (Thermo Electron, Waltham, MA, and Wako Diagnostic, Richmond, VA).

EE and locomotor activity. EE and home-cage activity were assessed using a combined indirect calorimetry system (TSE Systems, Chesterfield, MO) as previously described (18). O_2 consumption and CO_2 production were measured every 10 min to determine the respiratory quotient and EE. Home-cage locomotor activity was determined using a multidimensional infrared light-beam system expressed as beam breaks.

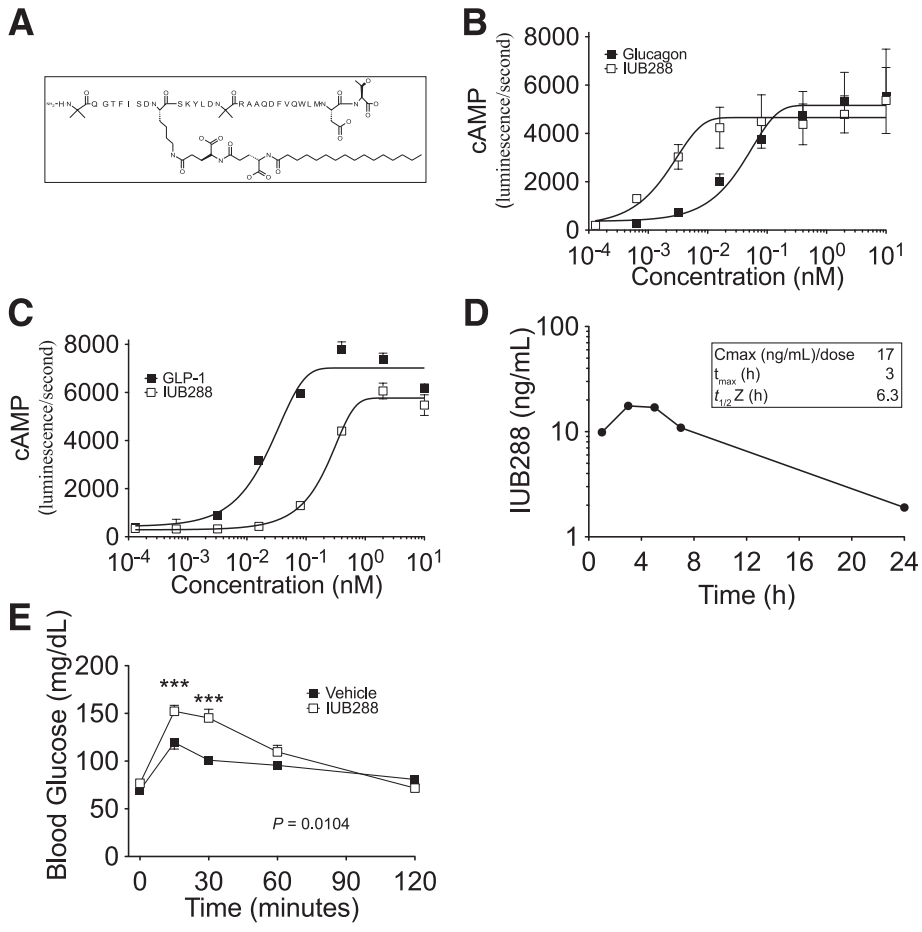

FIG. 1. Characteristics of the GcgR agonist IUB288. *A*: IUB288 chemical structure. Activity of IUB288 at the GcgR (*B*) and GLP-1 receptor (*C*) in cultured HEK293 cells. Dose-normalized bioavailability of IUB288 (*D*) after a single subcutaneous injection (10 nmol/kg) in C57Bl/6J mice (displayed as the mean of $n = 2$). Blood glucose excursion (*E*) in response to an acute IUB288 challenge (10 nmol/kg) in lean, chow-fed, male C57Bl/6J mice ($n = 8$ per treatment). All data are represented as mean ± SEM. ***$P < 0.001$ vs. vehicle control, two-way ANOVA with Bonferroni post hoc analysis.

Gene expression. Mice were decapitated without anesthesia, and trunk blood and tissues were collected immediately. Tissues were frozen on dry ice and stored at −80°C. RNA was isolated using the RNeasy Lipid Mini-Kit (Qiagen, Valencia, CA) according to the manufacturer's instructions. cDNA was synthesized by reverse transcription PCR using SuperScriptIII, DNase treatment, and anti-RNase treatment (Invitrogen, Carlsbad, CA). Single-gene qPCR was performed according to the manufacturer's instructions on a 7900 real-time PCR machine (Applied Biosystems, Foster City, CA). Data were normalized to the housekeeping gene 18s and expressed as fold change.

Cell culture. Primary hepatocytes were isolated as previously described (19). Rat H4IIE cells purchased from American Type Culture Collection (Manassas, VA) were cultured in Eagle's minimum essential medium (4.5 g/L glucose) containing 1% FBS (HyClone Laboratories, Grand Island, NY) and antibiotics (penicillin, 75 μg/mL; streptomycin, 50 μg/mL) in 5% CO_2/95% air at 37°C. Treatments were conducted when H4IIE cells reached 90% confluence in six-well plates.

Statistics. All data are represented as mean and SEM. Significance was determined by one-way or two-way ANOVA with Bonferroni multiple comparison posttest and, when appropriate, by unpaired Student *t* test. All statistics were performed using GraphPad Prism version 5.0 for Windows (GraphPad Software, San Diego, CA). Statistical significance was assumed when $P < 0.05$.

RESULTS

Development of a potent, soluble, long-acting, and selective GcgR agonist. Although discovered in the early 1920s, the native structure of glucagon has hindered in-depth investigation of its biology, as it does not easily lend itself to mechanistic pharmacological studies due to its low aqueous solubility (20) and its propensity to form amyloid-like fibrils (21). The dissection of functional interactions between glucagon and FGF21 in the regulation of systems metabolism therefore required the generation of a long-acting, soluble, and highly selective GcgR agonist. This objective was fulfilled by subtle modification of the glucagon sequence that extended its duration of action while maintaining selectivity. The chemical structure of IUB288 (HaibQGTFISDK[rErE-C16]SKYLDaibRAAQDFVQWLMDT) differs from native glucagon at six positions (Fig. 1*A*). Collectively, the in vitro receptor profile of this acylated glucagon agonist is shown in Fig. 1*B* and *C*, where IUB288 demonstrates activity sizably enhanced relative to native glucagon and a selectivity of approximately 100-fold at the GLP-1 receptor.

Subcutaneous injection (10 nmol/kg) of this GcgR agonist in naive C57Bl/6J mice resulted in a prolonged bioavailability over 24 h (Fig. 1*D*), with similar results observed in rats (data not shown). Peak concentration (C_{max}) and mean estimated terminal elimination half-life ($t_{1/2}$, z) at this dose were observed to be 17 ng/mL and 6.3 h, respectively. Further confirming its in vivo efficacy, intraperitoneal injection (10 nmol/kg) in C57Bl/6J mice significantly increased t = 15 and 30 min, as well as overall blood glucose ($P = 0.0104$) (Fig. 1*E*). Taken together, these data suggest that IUB288 is a potent, long acting, and selective GcgR agonist that may allow in vivo inspection of chronic GcgR signaling.

GcgR agonism promotes negative energy balance in DIO mice. To investigate the effect of chronically increased GcgR signaling on energy metabolism, we compared several levels of GcgR activation in DIO mice. GcgR agonism lowered body weight and food intake, with a significant decrease observed at an agonist dose of 10 nmol/kg (Fig. 2*A* and *B*).

The ad lib blood glucose in these mice increased in a dose-dependent manner (Fig. 2*C* and *D*). We next assessed the effect of chronic GcgR agonism in age-matched chow-fed and DIO mice. Daily treatment of these mice (10 nmol/kg/day) decreased body and fat mass in DIO but not in lean mice (Fig. 3*A* and *B* and Supplementary Fig. 1*G*). Food intake in the standard chow-fed mice was elevated (day 16, $P < 0.05$) after chronic GcgR activation as compared with vehicle-treated mice (Fig. 3*C*). Conversely, in DIO mice receiving chronic GcgR activation, there was no difference in food intake (Fig. 3*C*). In addition to its effects on body weight and fat mass, GcgR agonism rescued hypercholesterolemia, but not the

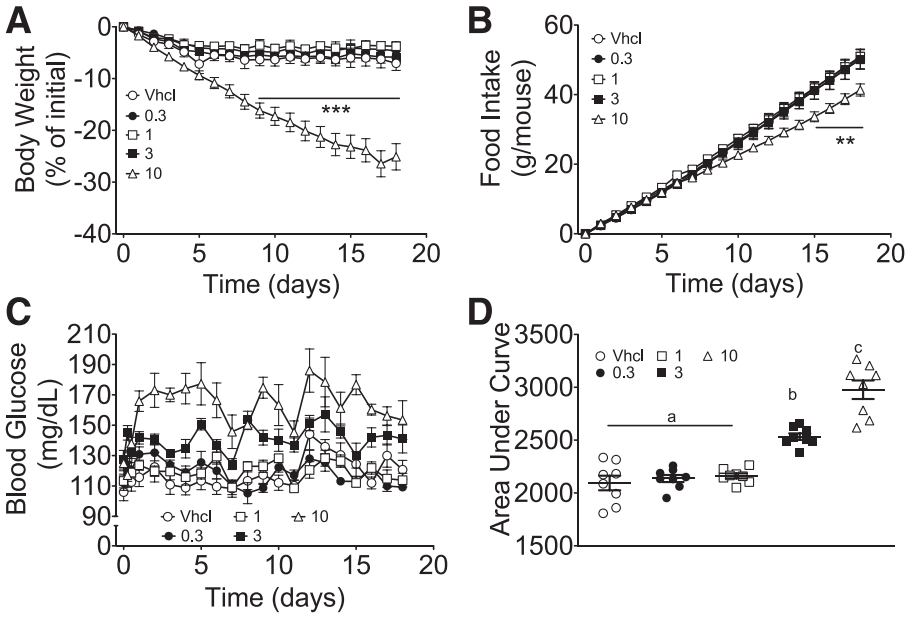

FIG. 2. Dose-dependency study of chronic GcgR activation. Body weight (*A*), food intake (*B*), and ad libitum blood glucose (*C* and *D*) in response to vehicle (PBS, ○) or 0.3 (●), 1.0 (□), 3.0 (■), or 10 nmol/kg/day (△) IUB288. All treatments were conducted in 11-month-old male C57Bl/6J mice maintained on HFD for 9 months. All data are represented as mean ± SEM; $n = 8$ per treatment. $^{**}P < 0.01$; $^{***}P < 0.001$ vs. vehicle control, two-way ANOVA with Bonferroni post hoc analysis. Lowercase letters (*D*) denote statistically similar ($P > 0.05$) groups, one-way ANOVA with Bonferroni post hoc analysis.

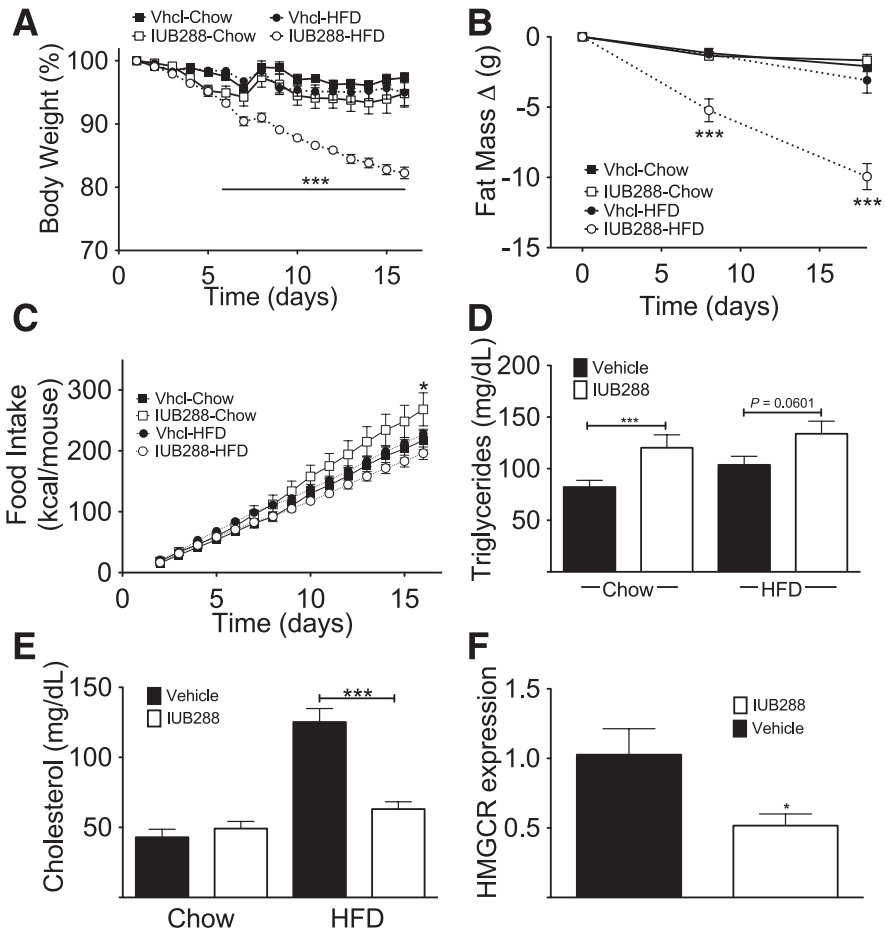

FIG. 3. Effects of chronic GcgR activation on energy balance and plasma lipids. Body weight (*A*), fat mass (*B*), and food intake (*C*) in response to 16 days of vehicle (PBS, closed symbols) or 10 nmol/kg/day IUB288 (open symbols) treatment in standard chow– (circles) or HFD-fed (squares) C57Bl/6J mice. Plasma concentrations of triglycerides (*D*) and cholesterol (*E*) and hepatic HMGCR expression (*F*) after 18 days of vehicle (PBS, closed bars) or 10 nmol/kg/day IUB288 (open bars) in standard chow– or HFD-fed C57Bl/6J mice. All treatments were conducted in 11-month-old male C57Bl/6J mice maintained on standard chow or HFD for 9 months. All data are represented as mean ± SEM; $n = 8$ per treatment. *A–C*: *$P < 0.05$; ***$P < 0.001$ vs. vehicle control, two-way ANOVA with Bonferroni post hoc analysis. *D* and *E*: ***$P < 0.001$ vs. vehicle control, one-way ANOVA with Bonferroni post hoc analysis. *F*: *$P < 0.05$ vs. vehicle control, unpaired Student *t* test.

hypertriglyceridemia observed in DIO mice (Fig. 3*D* and *E*). Consistent with the decrease in plasma cholesterol, hepatic 3-hydroxy-3-methylglutaryl coenzyme-A reductase (HMGCR) expression was suppressed by chronic GcgR activation in DIO mice (Fig. 3*F*). Both chow-fed and DIO groups demonstrated increased ad libitum blood glucose and impaired glucose tolerance when treated with IUB288 (Supplementary Fig. 1*A* and *B*). Chronic GcgR activation had no clear effect on plasma insulin, leptin, GLP-1, or endogenous glucagon levels in DIO mice (Supplementary Fig. 1*C–F*). Taken together, these data suggest that chronic GcgR activation affects glucose homeostasis, lipidemia, body weight, and food intake, although only the glycemic regulation was dose dependent in nature.

Glucagon-stimulated body and fat mass loss is leptin independent. To evaluate the role of leptin signaling in Gcg-stimulated loss of body and fat mass, we administered GcgR agonist to *db/db* mice for 7 days. Daily treatment of these mice (10 nmol/kg/day) stimulated a decrease in body weight (Fig. 4*A* and *B*) and increased core body temperature (Fig. 4*C*). Chronic GcgR agonism in hyperglycemic *db/db* mice did not affect ad lib or fasting blood glucose (Fig. 4*D* and *E*) but enhanced insulin sensitivity, as assessed by glucose excursion and rate of disappearance (Kd) during an intraperitoneal insulin tolerance test (Fig. 4*F* and *G*). Food intake was not different between treated and vehicle mice (Fig. 4*H*).

GcgR activation stimulates FGF21 expression and secretion in vivo. The metabolic action profile of FGF21, derived from the liver, pancreas, and adipose tissue (22), significantly overlaps with that of glucagon. To dissect the molecular mechanisms mediating the metabolic actions of Gcg R agonism in vivo, we tested the hypothesis that FGF21 may play a relevant role. We observed that acute Gcg Ractivation in DIO C57Bl/6J mice significantly increased plasma FGF21 (Fig. 5*A*). Mirroring the bioavailability of our GcgR agonist, this elevation in plasma FGF21 subsequently returned to baseline levels, suggesting that acute GcgR activation reversibly upregulates FGF21 secretion in rodents. When continued for 16 days, chronic GcgR activation increased both hepatic FGF21 expression (Fig. 5*B*) and plasma FGF21 (Fig. 5*C*). These elevated FGF21 levels coincided with a robust decrease in body weight and fat mass, as displayed in Fig. 2. These findings demonstrate that GcgR agonism stimulates FGF21 expression and secretion in association with glucagon-induced body and fat mass loss.

GcgR activation stimulates expression of FGF21 in vitro. As hepatocytes express both GcgR and FGF21, we next investigated if glucagon-stimulated FGF21 secretion

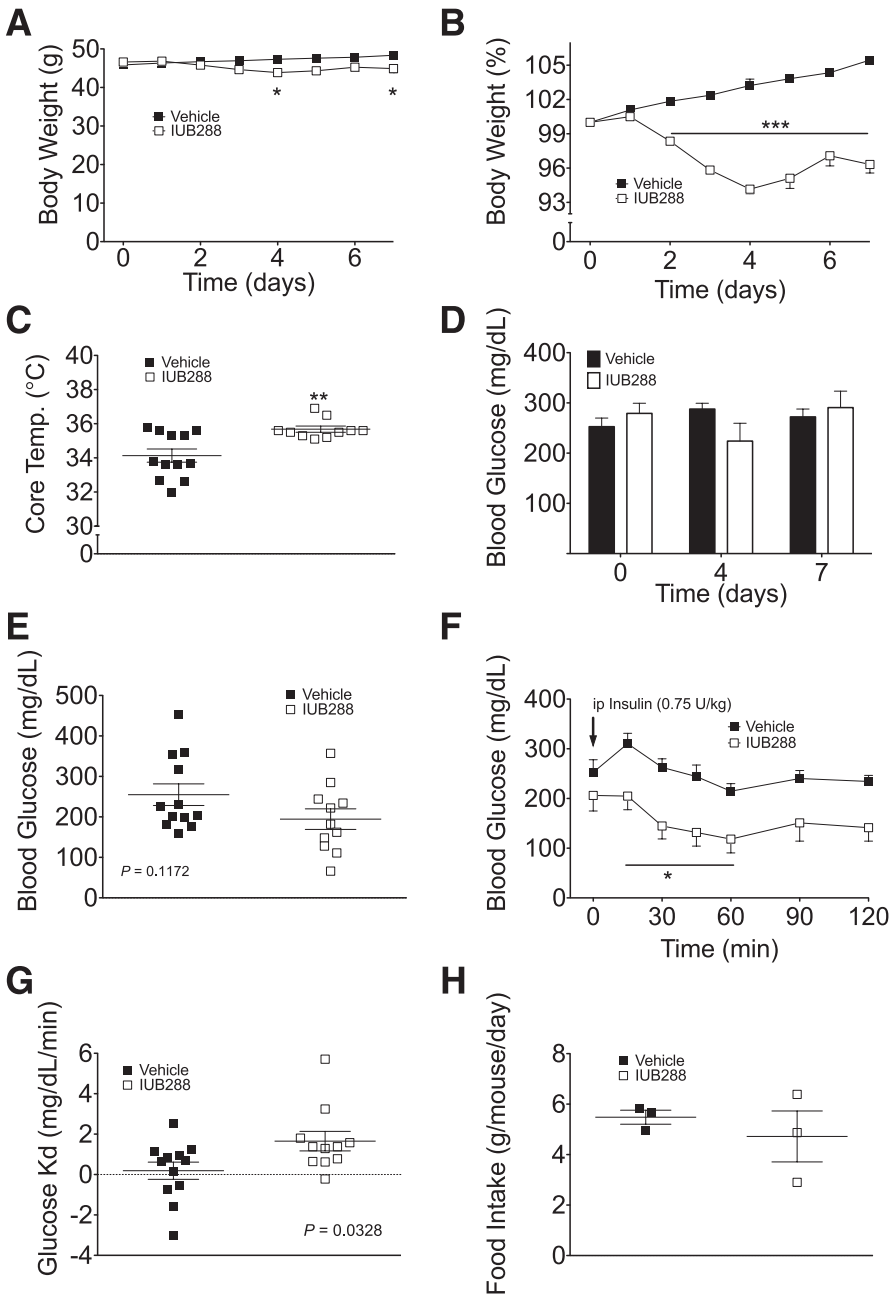

FIG. 4. Effects of chronic GcgR activation in *db/db* mice. Absolute (*A*) and relative body weight (*B*) of *db/db* mice during 7 days of vehicle (PBS, ■) or 10 nmol/kg/day IUB288 (□) treatment. Body core temperature (*C*) on day 6 of vehicle (PBS, ■) or 10 nmol/kg/day IUB288 (□). Ad libitum blood glucose during chronic GcgR activation (*D*). Fasting blood glucose (6 h) (*E*) of *db/db* mice after 7 days of chronic GcgR activation. Blood glucose excursion (*F*) and rate of disappearance (Kd, 0–45 min) during 0.75 units/kg insulin challenge (*G*) after 7 days of chronic GcgR activation in 6-h fasted *db/db* mice. Cumulative food intake (*H*) of *db/db* mice (three cages of four mice per cage) during 7 days of vehicle (PBS, ■) or 10 nmol/kg/day IUB288 (open squares) treatment. All treatments were conducted in 12-week-old male *db/db* mice maintained on standard chow diet. All data are represented as mean ± SEM; *n* = 11–12 per treatment. *A*, *B*, and *F*: *$P < 0.05$; ***$P < 0.001$ vs. vehicle control, two-way ANOVA with Bonferroni post hoc analysis. *C*: **$P < 0.01$ vs. vehicle control, unpaired Student *t* test.

could be induced in a cell-autonomous manner. We found that glucagon dose-dependently increased FGF21 expression and secretion in wild-type (WT) hepatocytes, but not GcgR knockout hepatocytes (Fig. 5*D* and *E*). Likewise, GcgR activation in rat H-4IIE cells stimulated FGF21 expression (Fig. 5*F*), indicating that GcgR activation triggers FGF21 production in a cell-autonomous manner.

Native glucagon stimulates FGF21 secretion in humans. To evaluate if these results are clinically relevant, we next administered native glucagon (1 mg) to 12 obese, healthy human volunteers. Plasma FGF21 concentrations increased significantly (Fig. 5*G*) after glucagon administration. In contrast, plasma FGF21 concentrations slightly decreased (240 min) after placebo administration. The area under the curve for glucagon-induced FGF21 secretion over time was significantly greater when compared with placebo (Fig. 5*H*).

Protection from diet-induced obesity by chronic GcgR activation requires FGF21. To test the hypothesis that FGF21 mediates the metabolic effects of glucagon, we

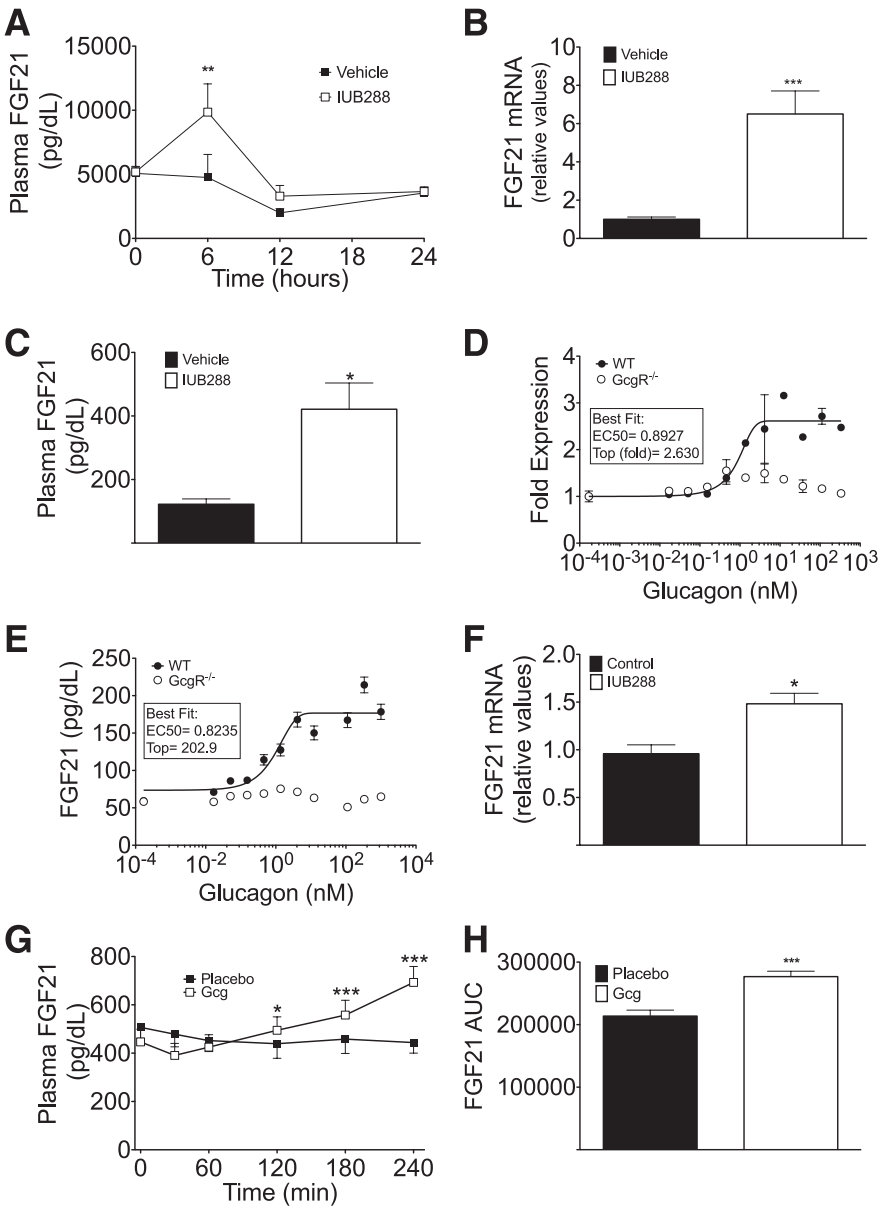

FIG. 5. Glucagon as an FGF21 secretagogue. Plasma FGF21 concentration (*A*) in response to acute GcgR activation (n = 8; 10 nmol/kg IUB288). Hepatic FGF21 expression (*B*) and plasma FGF21 concentration (*C*) after 18 days of vehicle (PBS, closed bars) or 10 nmol/kg/day IUB288 (open bars) in 2-h fasted, HFD-fed mice (n = 4–5). Relative FGF21 expression (*D*) and secretion (*E*) in isolated primary hepatocytes from WT and GcgR knockout ($GcgR^{-/-}$) mice after 9.5 and 25 h glucagon treatment, respectively. Relative FGF21 expression in cultured H4IIE cells (*F*) after 120 min GcgR activation (0.133 nmol/mL IUB288). Plasma FGF21 concentration (*G*) and area under the curve (AUC) analysis (*H*) after glucagon challenge (1 mg) in human subjects. Data from *A*–*C* obtained in 11-month-old male C57Bl/6J mice maintained on HFD for 9 months. All data are represented as mean ± SEM. *A* and *G*: *$P < 0.05$; **$P < 0.01$; ***$P < 0.001$ vs. vehicle control, two-way ANOVA with Bonferroni post hoc analysis. *B*, *C*, *F*, and *H*: *$P < 0.05$; ***$P < 0.001$ vs. vehicle control, unpaired Student t test. *D* and *E*: Sigmoidal dose-response best fit (with variable slope).

activated GcgR in age-matched FGF21-deficient ($FGF21^{-/-}$) and WT mice (10 nmol/kg/day). Acute challenge with the GcgR agonist increased blood glucose over a 60-min period, regardless of genotype (Supplementary Fig. 2*A*). Chronic GcgR activation in WT mice prevented body weight accrual in mice switched to HFD on day 0 (Fig. 6*A*); however, this effect was ablated in mice deficient for FGF21 (Fig. 6*B*). Chronic GcgR activation also prevented fat mass accumulation in WT mice (Fig. 6*C*), but not in $FGF21^{-/-}$ mice (Fig. 6*D*). Lean mass was slightly, but significantly, reduced in WT mice, but not in $FGF21^{-/-}$ mice (Fig. 6*E* and *F*). Food intake did not differ between genotype or treatment groups (Fig. 6*G*), consistent with the previous reports that GcgR activation may predominantly affect chronic energy balance via modulation of EE (reviewed in 23,24). Consistent with the effects in DIO WT mice (Fig. 4), chronic GcgR activation triggered a robust increase in hepatic expression and plasma FGF21 of WT mice, whereas, predictably, FGF21 levels in $FGF21^{-/-}$ mice were not detectable (Supplementary Fig. 2*B* and *C*).

Increased EE in response to GcgR activation requires FGF21. To evaluate the direct contribution of FGF21 to GcgR-induced effects on EE, we next treated WT and $FGF21^{-/-}$ mice inside an indirect calorimeter. After 24 h of acclimation, WT and the $FGF21^{-/-}$ mice were injected

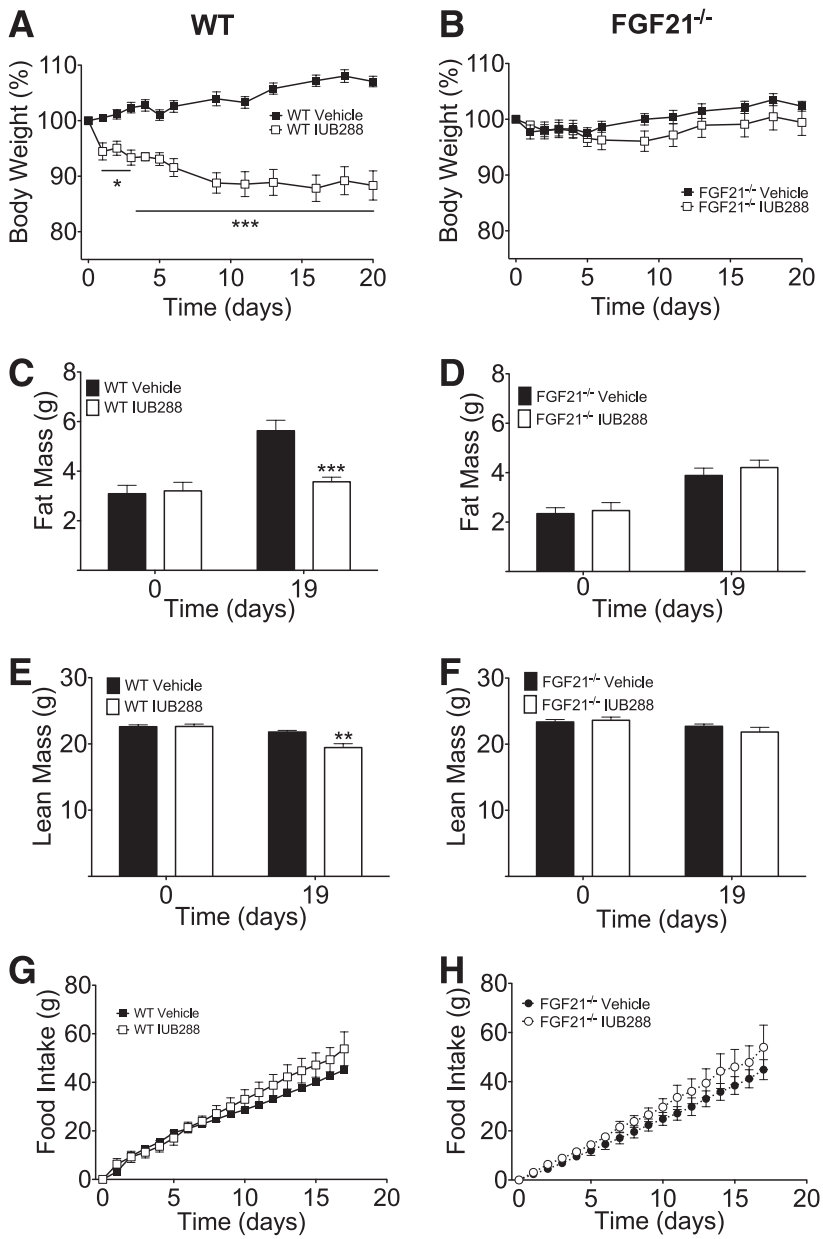

FIG. 6. Energy balance during chronic GcgR activation in *FGF21*$^{-/-}$ mice. Body weight, fat mass, lean mass, and food intake of WT (*A*, *C*, *E*, and *G*) and *FGF21*$^{-/-}$ (*B*, *D*, *F*, and *H*) mice during 20 days of vehicle (PBS, closed symbols) or 10 nmol/kg/day IUB288 (open symbols) treatment. All treatments were conducted in 12-week-old male littermates maintained on standard chow diet until day 0 and then switched to HFD upon initiation of GcgR activation. All data are represented as mean ± SEM; n = 12–16. *$P < 0.05$; **$P < 0.01$; ***$P < 0.001$ vs. genotype-specific vehicle control, two-way ANOVA with Bonferroni post hoc analysis.

with IUB288 (10 nmol/kg/day) or vehicle. WT mice increased EE in response to chronic GcgR agonism (Fig. 7*A* and *C*), whereas *FGF21*$^{-/-}$ mice were unaffected by the treatment (Fig. 7*B* and *D*). The changes in EE observed in WT mice were associated with an increase in spontaneous locomotor activity, whereas no effects on locomotor activity were observed in *FGF21*$^{-/-}$ mice (Fig. 7*E* and *F*).

Glucose and lipid metabolism changes caused by chronic GcgR activation partially require FGF21. Chronic GcgR agonism potentiates hepatic and adipocyte lipolysis while reducing plasma cholesterol (23). Interestingly, chronic GcgR activation lowered circulating cholesterol in WT mice, but not in *FGF21*$^{-/-}$ mice (Fig. 8*A*). Liver triglycerides were unaffected in either genotype (Fig. 8*B*). The effects of GcgR agonism on plasma triglycerides (Fig. 8*C*) and NEFAs (Fig. 8*D*) were potentiated in *FGF21*$^{-/-}$ mice.

The hyperglycemia induced by chronic GcgR agonism in WT mice was blunted in *FGF21*$^{-/-}$ mice (Fig. 8*E*). Furthermore, chronic GcgR activation induced glucose intolerance in both WT and *FGF21*$^{-/-}$ mice as compared with matched vehicle-treated controls (Fig. 8*F* and *G*). Interestingly, vehicle-treated *FGF21*$^{-/-}$ mice exhibited better glucose tolerance than vehicle-treated WT mice, as assessed by intraperitoneal glucose challenge (Fig. 8*E* and *F*). Taken together, these data suggest that FGF21 is required for some, but not all, GcgR-mediated effects on glucose and lipid metabolism.

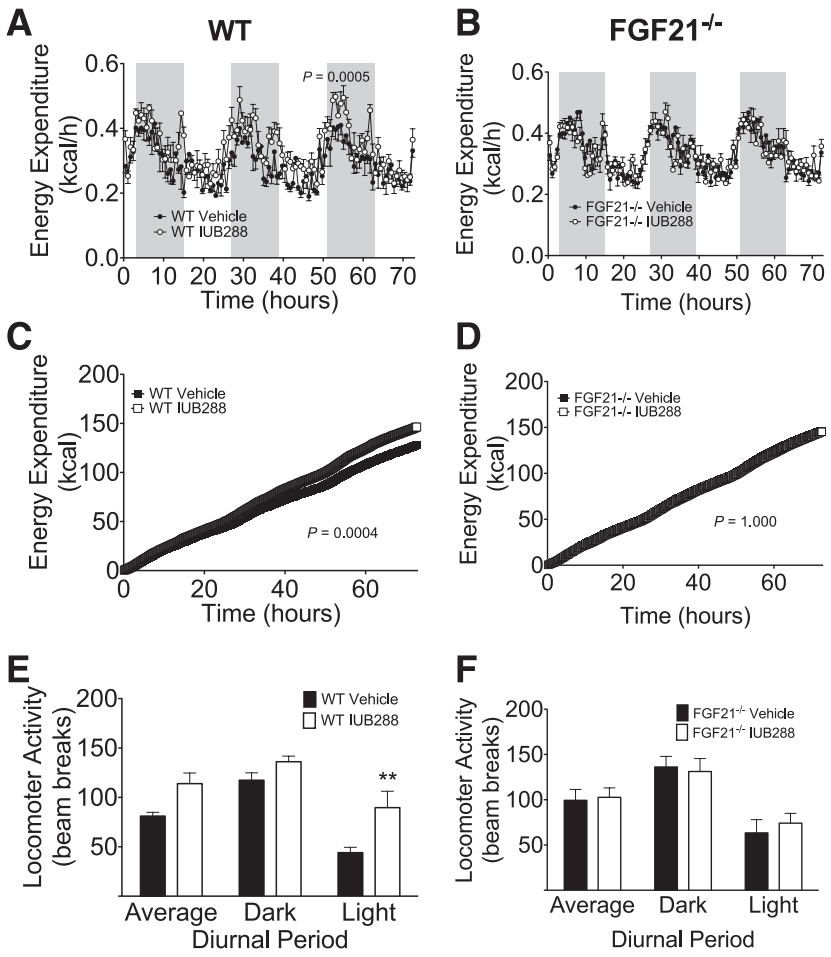

FIG. 7. EE during chronic GcgR activation. Dynamic and cumulative EE and locomotor activity of WT (*A*, *C*, and *E*) and *FGF21*$^{-/-}$ (*B*, *D*, and *F*) mice during 72 h of vehicle (PBS, closed symbols) or 10 nmol/kg/day IUB288 (open symbols) treatment. All treatments were conducted in 12-week-old male littermates maintained on standard chow diet. IUB288 or vehicle administered daily, 2 h prior to dark phase. *P* values of *A–C* denote main effect of treatment vs. vehicle control by two-way ANOVA. All data are represented as mean ± SEM; *n* = 6. *E*: ***P* < 0.01 vs. genotype-specific vehicle control, two-way ANOVA with Bonferroni post hoc analysis.

DISCUSSION

Glucagon is an integral component of the adaptive response to fasting in mammals, stimulating hepatic glucose production while concomitantly liberating lipid energy stores to maintain energy homeostasis. However, the molecular properties of native glucagon (20,21) have historically made detailed investigation of this hormone an arduous task. Here we report the discovery of a long-acting, soluble, and highly selective GcgR agonist (IUB288). We have successfully used this acylated glucagon agonist for chronic activation of GcgR signaling in vivo as a means to probe glucagon biology. Data from these studies suggest that chronic GcgR agonism suppresses plasma cholesterol while stimulating hyperglycemia and fat mass loss. Chronic activation of GcgR also elevated hepatic FGF21 expression and secretion. Genetic deletion identified FGF21 as an essential mediator for the majority of glucagon's long-term metabolic effects.

Development of a potent, soluble, long-acting, and selective GcgR agonist. The GcgR agonist IUB288 is characterized by several important substitutions, resulting in a potent, soluble, long-acting, and selective GcgR agonist. The aib at position 2 is used to minimize proteolytic degradation by dipeptidyl peptidase-4, a factor that is of increased importance given its extended duration of action. Substitution of the native Thr with Ile at position 7 maximizes GcgR selectivity by lessening potency at the GLP-1 receptor. The acylation at position 10 with a linear dipeptide of γ-Glu capped with a C16 fatty acid provided the optimal aqueous solubility and suitability for once-a-day administration as a subcutaneous injection. Aib16 stabilizes the backbone of the peptide, maximizing receptor potency and chemical stability by elimination of the native Asp-Ser sequence, which is prone to chemical rearrangement. This single change is of utmost importance in minimizing the propensity to form an amyloid-like structure. The Arg to Ala substitution at position 18 minimizes potential degradation, given the propensity of dibasic amino acids to plasma proteolysis. Finally, the change of Asn28 to Asp increases the chemical stability of the peptide and further enhances aqueous solubility. In sum, these augmentations result in a highly potent and selective agonist with dramatically extended bioavailability. The liver and kidneys rapidly clear circulating native glucagon (25,26). Reports from humans and dogs suggest that the half-life of this hormone is 5–6 min (26,27). Thus, it can be approximated that our GcgR agonist displays a mean estimated terminal elimination half-life that is 63-fold longer than that of native glucagon.

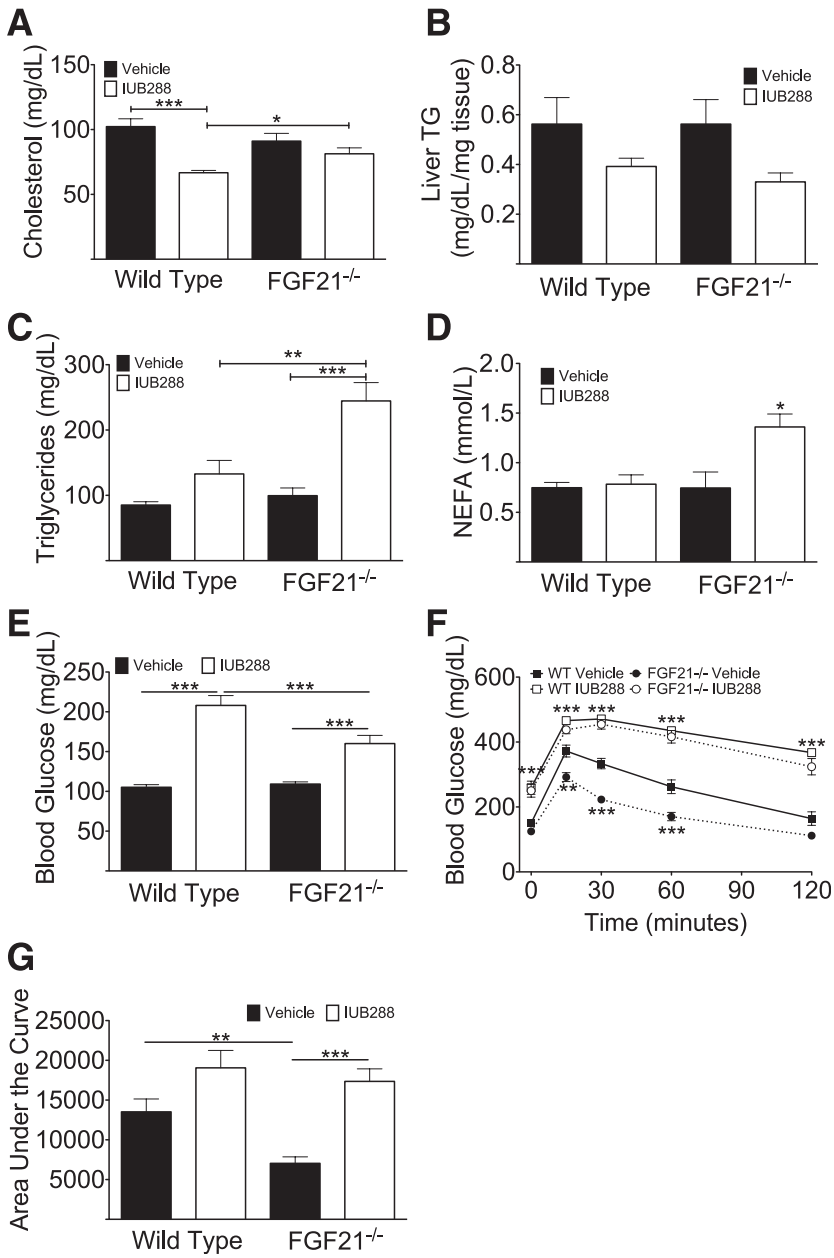

FIG. 8. Lipidemia and glycemia during chronic GcgR activation. Liver triglyceride (*B*) and plasma cholesterol (*A*), triglyceride (*C*), and NEFA (*D*) concentrations of WT and *FGF21*$^{-/-}$ mice after 20 days of vehicle (PBS, closed symbols) or 10 nmol/kg/day IUB288 (open symbols) treatment (n = 4–6). Ad libitum blood glucose (*E*) of WT and *FGF21*$^{-/-}$ mice on day 19. Glucose tolerance (*F*) (as assessed by 1.5 g/kg intraperitoneal glucose challenge) and area under the curve analysis (*G*) of WT (squares) and *FGF21*$^{-/-}$ (circles) mice after 19 days of vehicle (PBS, closed symbols) or 10 nmol/kg/day IUB288 (open symbols) treatment (n = 12–16). All treatments conducted in 12-week-old male littermates maintained on standard chow diet until day 0 and then switched to HFD upon initiation of GcgR activation. All data are represented as mean ± SEM. *P < 0.05; **P < 0.01; ***P < 0.001 vs. genotype-specific vehicle control, two-way ANOVA with Bonferroni post hoc analysis. *F*: **P < 0.01; ***P < 0.001 vs. WT vehicle control, two-way ANOVA with Bonferroni post hoc analysis.

Glucagon and lipidemia. A growing body of evidence suggests that glucagon represents a relevant regulator of lipid metabolism. Mechanistically, it has been suggested that glucagon signaling may suppress expression of HMGCR (28), the rate-limiting enzyme in cholesterol synthesis. Although we observed decreased HMGCR in WT mice, it is important to note that the decreased cholesterolemia in WT mice was not observed in mice lacking FGF21.

GcgR agonism stimulates body and fat mass loss in DIO mice. Studies over the past five decades have reported glucagon-stimulated body weight loss in both humans (29) and rodents (30). However, this phenomenon received limited attention until we and others recently reported potent body weight–lowering effects of novel single-molecule coagonists combining GLP-1 and glucagon agonism (7,8). Results from our study suggest that glucagon action stimulates a loss of body mass that is primarily a consequence of decreased fat mass, although a subtle decrease in lean mass was observed in some experiments. Multiple mechanisms for glucagon-stimulated body weight loss have been put forth, including altered energy balance (reviewed in 23,24). Studies described herein suggest that increased EE may be the predominant physiological mechanism for GcgR-induced body weight loss.

Glucagon-stimulated negative energy balance is leptin independent. The rapid and considerable body and fat mass loss concomitant to increased EE resembled the consequences of increased leptin signaling. To test the hypothesis that GcgR signaling enhances leptin signaling and/or sensitivity, we assessed the effect of chronic GcgR agonism in a model lacking leptin signaling (*db/db* mice). Contrary to our initial hypothesis, our data suggest that chronic GcgR agonism stimulates body weight loss and increases core temperature independent of leptin signaling. However, unlike the further impaired glucose tolerance observed in DIO and chow-fed mice, GcgR-activated *db/db* mice displayed an unexpected enhancement in insulin action.

Glucagon and FGF21. These observations led us to investigate regulators of EE that may also represent downstream targets of glucagon signaling. Our data support the hypothesis that glucagon-stimulated loss of body fat may be mediated through FGF21. We find that both native glucagon and our GcgR agonist increase FGF21 secretion in rodents and humans. Importantly, this effect is retained in isolated primary hepatocytes from WT mice, but not GcgR knockout mice, suggesting that GcgR signaling in hepatocytes directly stimulates FGF21 expression and secretion. Our studies also highlight a role for FGF21 in the majority of effects triggered by chronic glucagon action. Using *FGF21*$^{-/-}$ mice, we discovered that FGF21 is essential for, and may directly mediate, glucagon regulation of body weight, fat mass, and plasma cholesterol. FGF21 is also essential for the increased EE observed during chronic GcgR agonism that is coupled with increased locomotor activity. This increase in activity is particularly pronounced in the light phase. Although much is known concerning GcgR agonism and EE, its effect on locomotor activity is not well described. Though consistent with an increased overall EE (23,24), our findings are in direct conflict with a prior report (31) and, as such, deserve continued investigation. Importantly, these effects are observed during chronically increased GcgR agonism. Conversely, the acute effects of glucagon action on glycemia are still observed in the absence of FGF21. Taken together, our results suggest that glucagon signaling stimulates FGF21 expression and secretion in order to achieve its long-term effects on energy and lipid and glucose metabolism.

FGF21 and glucose homeostasis. These studies unexpectedly suggest that GcgR-induced hyperglycemia is blunted in mice lacking FGF21. FGF21 pharmacology reduces hyperglycemia, dyslipidemia, and plasma glucagon in diabetic mice and nonhuman primates (9). These effects were accompanied by increased insulin secretion and sensitivity (32), building upon a prior body of work detailing the antidiabetic effects of FGF21 (9,33–36). It is possible that the explanation for this discrepancy lies in an off-target effect of our agonist or uncoupling of the glucagon-FGF21 axis at the level of glucose regulation. However, a deeper understanding of the multiple and complex roles of FGF21 will be required to reconcile all available findings and pave the way for optimal selection of potential therapeutic strategies.

In summary, we report a mechanism linking two of today's most promising target pathways for the treatment of diabetes and obesity: glucagon and FGF21. This link appears to be liver-cell autonomous and conserved through species. Our discovery sheds new light on the emerging suitability of key fasting response elements as target pathways for the treatment of metabolic disease and may also explain the well-known wasting syndrome observed in patients suffering from glucagon-producing tumors (37). Future studies, including GcgR loss of function, will allow us to further dissect the detailed molecular interactions connecting glucagon and FGF21 action and may provide additional drug targets for the treatment of both cancer-related wasting syndromes and diet-induced metabolic diseases such as obesity and type 2 diabetes.

ACKNOWLEDGMENTS

This work was supported by research funds from Marcadia Biotech and Roche Pharmaceuticals. M.H.T. has served as a consultant for Roche Pharmaceuticals and has received Roche research funds. R.D.D., R.J.S., and D.P.-T. have a collaborative association with Roche Research Laboratories pertaining to peptide-based therapeutics in metabolism. A.Kh. and C.C. are employees of Eli Lilly and Co. A.Ko, S.B., and M.Ka. are employees of F. Hoffmann-La Roche Ltd. No other potential conflicts of interest relevant to this article were reported.

K.M.Ha., R.D.D., and M.H.T. conceived, implemented, and designed the study, analyzed and interpreted data, and drafted the article and revised it critically. K.S. and C.C. implemented the study and analyzed and interpreted data. T.D.M., A.M.A., M.Ko., S.C.W., S.M.H., D.D., P.T.P., D.P.-T., R.J.S., N.I., A.Kh., and J.S. interpreted data and drafted the article and revised it critically. K.M.He., N.O., J.H., J.L.H., R.K., A.Ko., S.B., and M.Ka. implemented the study. D.S. and V.G. implemented the study, interpreted data, and drafted the article and revised it critically. All authors approved the final version of the manuscript to be published. M.H.T. is the guarantor of this work and, as such, had full access to all the data in the study and takes responsibility for the integrity of the data and the accuracy of the data analysis.

Parts of this study were presented at the 72nd Scientific Sessions of the American Diabetes Association, Philadelphia, Pennsylvania, 8–12 June 2012.

The authors would like to thank Darleen Sandoval (University of Cincinnati) for valuable discussions and advice. The authors would also like to thank Christophe Flament (F. Hoffmann-La Roche Ltd.) for his assistance in the technical measurements of IUB288.

REFERENCES

1. Quesada I, Todorova MG, Soria B. Different metabolic responses in alpha-, beta-, and delta-cells of the islet of Langerhans monitored by redox confocal microscopy. Biophys J 2006;90:2641–2650
2. Gu W, Yan H, Winters KA, et al. Long-term inhibition of the glucagon receptor with a monoclonal antibody in mice causes sustained improvement in glycemic control, with reversible alpha-cell hyperplasia and hyperglucagonemia. J Pharmacol Exp Ther 2009;331:871–881
3. Wang MY, Chen L, Clark GO, et al. Leptin therapy in insulin-deficient type I diabetes. Proc Natl Acad Sci USA 2010;107:4813–4819
4. Brown RJ, Sinaii N, Rother KI. Too much glucagon, too little insulin: time course of pancreatic islet dysfunction in new-onset type 1 diabetes. Diabetes Care 2008;31:1403–1404
5. Dunning BE, Gerich JE. The role of alpha-cell dysregulation in fasting and postprandial hyperglycemia in type 2 diabetes and therapeutic implications. Endocr Rev 2007;28:253–283
6. Gromada J, Franklin I, Wollheim CB. Alpha-cells of the endocrine pancreas: 35 years of research but the enigma remains. Endocr Rev 2007;28:84–116
7. Day JW, Ottaway N, Patterson JT, et al. A new glucagon and GLP-1 coagonist eliminates obesity in rodents. Nat Chem Biol 2009;5:749–757
8. Pocai A, Carrington PE, Adams JR, et al. Glucagon-like peptide 1/glucagon receptor dual agonism reverses obesity in mice. Diabetes 2009;58:2258–2266

9. Kharitonenkov A, Wroblewski VJ, Koester A, et al. The metabolic state of diabetic monkeys is regulated by fibroblast growth factor-21. Endocrinology 2007;148:774–781
10. Inagaki T, Dutchak P, Zhao G, et al. Endocrine regulation of the fasting response by PPARalpha-mediated induction of fibroblast growth factor 21. Cell Metab 2007;5:415–425
11. Badman MK, Pissios P, Kennedy AR, Koukos G, Flier JS, Maratos-Flier E. Hepatic fibroblast growth factor 21 is regulated by PPARalpha and is a key mediator of hepatic lipid metabolism in ketotic states. Cell Metab 2007;5: 426–437
12. Lundåsen T, Hunt MC, Nilsson LM, et al. PPARalpha is a key regulator of hepatic FGF21. Biochem Biophys Res Commun 2007;360:437–440
13. Berglund ED, Kang L, Lee-Young RS, et al. Glucagon and lipid interactions in the regulation of hepatic AMPK signaling and expression of PPARalpha and FGF21 transcripts in vivo. Am J Physiol Endocrinol Metab 2010;299: E607–E614
14. Kharitonenkov A, Shiyanova TL, Koester A, et al. FGF-21 as a novel metabolic regulator. J Clin Invest 2005;115:1627–1635
15. Ito S, Fujimori T, Furuya A, Satoh J, Nabeshima Y, Nabeshima Y. Impaired negative feedback suppression of bile acid synthesis in mice lacking betaKlotho. J Clin Invest 2005;115:2202–2208
16. Arafat AM, Perschel FH, Otto B, et al. Glucagon suppression of ghrelin secretion is exerted at hypothalamus-pituitary level. J Clin Endocrinol Metab 2006;91:3528–3533
17. Hotta Y, Nakamura H, Konishi M, et al. Fibroblast growth factor 21 regulates lipolysis in white adipose tissue but is not required for ketogenesis and triglyceride clearance in liver. Endocrinology 2009;150: 4625–4633
18. Kirchner H, Hofmann SM, Fischer-Rosinsky A, et al. Caloric restriction chronically impairs metabolic programming in mice. Diabetes 2012;61: 2734–2742
19. Guo Y, Jolly RA, Halstead BW, et al. Underlying mechanisms of pharmacology and toxicity of a novel PPAR agonist revealed using rodent and canine hepatocytes. Toxicol Sci 2007;96:294–309
20. Desbuquois B, Aurbach GD. Effects of iodination on the distribution of peptide hormones in aqueous two-phase polymer systems. Biochem J 1974;143:83–91
21. Beaven GH, Gratzer WB, Davies HG: Formation and structure of gels and fibrils from glucagon. Eur J Biochem 1969;11:37–42
22. Kharitonenkov A, Larsen P. FGF21 reloaded: challenges of a rapidly growing field. Trends Endocrinol Metab 2011;22:81–86
23. Habegger KM, Heppner KM, Geary N, Bartness TJ, DiMarchi R, Tschöp MH. The metabolic actions of glucagon revisited. Nat Rev Endocrinol 2010; 6:689–697
24. Heppner KM, Habegger KM, Day J, et al. Glucagon regulation of energy metabolism. Physiol Behav 2010;100:545–548
25. Hinke SA, Pospisilik JA, Demuth HU, et al. Dipeptidyl peptidase IV (DPIV/CD26) degradation of glucagon. Characterization of glucagon degradation products and DPIV-resistant analogs. J Biol Chem 2000;275:3827–3834
26. Jaspan JB, Polonsky KS, Lewis M, et al. Hepatic metabolism of glucagon in the dog: contribution of the liver to overall metabolic disposal of glucagon. Am J Physiol 1981;240:E233–E244
27. Alford FP, Bloom SR, Nabarro JD. Glucagon metabolism in man, studies on the metabolic clearance rate and the plasma acute disappearance time of glucagon in normal and diabetic subjects. J Clin Endocrinol Metab 1976; 42:830–838
28. Edwards PA, Lan SF, Fogelman AM. The effect of glucagon on the synthesis and degradation of 3-hydroxy-3-methylglutaryl coenzyme A reductase. J Lipid Res 1986;27:398–403
29. Schulman JL, Carleton JL, Whitney G, Whitehorn JC. Effect of glucagon on food intake and body weight in man. J Appl Physiol 1957;11:419–421
30. de Castro JM, Paullin SK, DeLugas GM. Insulin and glucagon as determinants of body weight set point and microregulation in rats. J Comp Physiol Psychol 1978;92:571–579
31. Morawska D, Sieklucka-Dziuba M, Kleinrok Z. Central action of glucagon. Pol J Pharmacol 1998;50:125–133
32. Mu J, Pinkstaff J, Li Z, et al. FGF21 analogs of sustained action enabled by orthogonal biosynthesis demonstrate enhanced antidiabetic pharmacology in rodents. Diabetes 2012;61:505–512
33. Berglund ED, Li CY, Bina HA, et al. Fibroblast growth factor 21 controls glycemia via regulation of hepatic glucose flux and insulin sensitivity. Endocrinology 2009;150:4084–4093
34. Xu J, Lloyd DJ, Hale C, et al. Fibroblast growth factor 21 reverses hepatic steatosis, increases energy expenditure, and improves insulin sensitivity in diet-induced obese mice. Diabetes 2009;58:250–259
35. Sarruf DA, Thaler JP, Morton GJ, et al. Fibroblast growth factor 21 action in the brain increases energy expenditure and insulin sensitivity in obese rats. Diabetes 2010;59:1817–1824
36. Coskun T, Bina HA, Schneider MA, et al. Fibroblast growth factor 21 corrects obesity in mice. Endocrinology 2008;149:6018–6027
37. Mallinson CN, Bloom SR, Warin AP, Salmon PR, Cox B. A glucagonoma syndrome. Lancet 1974;2:1–5